

# Nanoscale

Accepted Manuscript



This is an *Accepted Manuscript*, which has been through the Royal Society of Chemistry peer review process and has been accepted for publication.

*Accepted Manuscripts* are published online shortly after acceptance, before technical editing, formatting and proof reading. Using this free service, authors can make their results available to the community, in citable form, before we publish the edited article. We will replace this *Accepted Manuscript* with the edited and formatted *Advance Article* as soon as it is available.

You can find more information about *Accepted Manuscripts* in the [Information for Authors](#).

Please note that technical editing may introduce minor changes to the text and/or graphics, which may alter content. The journal's standard [Terms & Conditions](#) and the [Ethical guidelines](#) still apply. In no event shall the Royal Society of Chemistry be held responsible for any errors or omissions in this *Accepted Manuscript* or any consequences arising from the use of any information it contains.

# Nanoparticle Hardness Controls the Internalization Pathway for Drug Delivery

Ye Li, Xianren Zhang and Dapeng Cao

*State Key Laboratory of Organic-Inorganic Composites, Beijing University of Chemical*

*Technology, Beijing 100029, China*

## Abstract

Nanoparticle (NP)-based drug delivery systems offer fundamental advantages over current therapeutic agents that commonly display longer circulation time, lower toxicity, specific targeted release, and greater bioavailability. For successful NP-based drug delivery it is essential that the drug-carrying nanocarriers can be internalized by target cells and transported to specific sites, and inefficient internalization of the nanocarriers is often one of major sources for drug resistance. In this work, we use the dissipative particle dynamics simulation to investigate the effect of NP hardness on their internalization efficiency. Three simplified models of NP platforms for drug delivery, including polymeric NP, liposome and solid NP, are designed here to represent increasing nanocarrier hardness. Simulation results indicate that NP hardness controls the internalization pathway for drug delivery. Rigid NPs can enter cell by a pathway of endocytosis, whereas for soft NP the endocytosis process can be inhibited or frustrated due to the wrapping-induced shape deformation and nonuniform ligand distribution. Instead, soft NPs tend to find one of three penetration pathways to enter the cell membrane via rearranging their hydrophobic and hydrophilic segments. Finally, we show that the interaction between nanocarriers and drug molecules is also essential for effective drug delivery.

**Keywords:** Endocytosis; penetration; drug delivery; dissipative particle dynamics simulation; nanoparticle hardness

## 1. Introduction

Traditional therapeutic agents show several limitations, such as off-target effect, poor water solubility, short circulation time, inconsistent stability, unfavorable biodistribution. As a comparison, nanoparticle (NP)-based drug delivery systems have shown significant promise in the development of drugs delivery systems that might overcome such limitations and address urgent needs to improve efficacy of diagnosis and therapy of various diseases. In the delivery systems, the free drug molecules could be encapsulated inside NPs, and enter into cells by the assistance of NPs. The drug molecules are then released from NPs after they have been delivered into the cytoplasm. For example, various NP-based approaches have been investigated to overcome the multidrug resistance developed by tumor cells, and one would expect a significant improvement in drug efficacy.<sup>1-4</sup> However, the poor cellular uptake remains a rate-limiting step for reaching the drug concentration level within the therapeutic window.<sup>5</sup> In many cases, therefore, understanding the interaction mechanisms of NPs with cell membranes and the key factors of controlling their uptake is of critical importance for cellular physiology and modern biomedicine.

For the NP uptake, there exist two internalization pathways: one is passive physical penetration of NPs with a size of several nanometers,<sup>6-9</sup> and the other is active endocytosis.<sup>10-16</sup> Both experimental and theoretical investigations show that the NP size,<sup>17-21</sup> shape,<sup>10, 22-24</sup> surface chemistry<sup>22-28</sup> and ligand arrangement<sup>8, 29, 30</sup> affect its active endocytosis or passive penetration.

Another property of NPs, which may influence their nanomedicine applications but have rarely investigated comparatively, is NP hardness or softness. NPs can be categorized with respect to their hardness. For example, metal or carbon-based NPs are considered “hard”, while dendrimer-, protein- or polymer-based NPs are

categorized as soft NPs. There exist another type of NPs that combine hard core and a soft shell.

The effect of NP hardness on the NP-membrane interaction, especially on drug delivery is nearly unexplored. Nevertheless, NP hardness seems to be another important factor affecting its internalization, which is often a crucial step for successful targeted drug delivery. This point can be inferred from following studies. Experimentally, Tao and Desai have found that macrophages are unable to phagocytose soft biological substances, which has profound implications on the functioning of the immune system.<sup>31</sup> Beningo and Wang have shown that phagocytosis of soft microparticles can be hindered by particle deformation.<sup>32</sup> Theoretically, Yi and Gao<sup>33</sup> and Ding and Ma<sup>30</sup> found that soft particles can hardly achieve full wrapping. Besides a recent theoretical work also showed that rod-shaped elastic nanoparticles can exhibit a similar elasticity-dependent effect on cell uptake,<sup>34</sup> and consistently, our previous simulation results indicated that endocytosis of soft vesicle becomes rather difficult.<sup>35</sup>

Based on above studies, we put forward here the idea that for drug delivery, NP hardness can be used to control the pathways for NP uptake, and emphasize the importance of nanocarrier hardness on achieving high drug efficacy. In clinical research, an increasing number of NP-based carriers, such as polymeric NPs,<sup>36-38</sup> liposomes,<sup>39-41</sup> dendrimers,<sup>42</sup> nanoemulsions<sup>43</sup> and metal NPs,<sup>44</sup> are used in drug delivery systems. It is well accepted now that in many cases overall efficacy of nanocarriers in overcoming drug resistance are marginal, and it is the poor endocytosis of nanocarriers that limits their potential. For example, Kunjachan et al. investigated different NP formulations, such as liposomes, polymers and micelles, to overcome multidrug resistance in four different cell lines (A431, SW620, B16-F10

and CT26) in drug-sensitive and drug-resistant form. It was found that the soft carrier materials did manage to overcome multidrug resistance to some extent, but that the overall benefit was quite small.<sup>45</sup> At least partially, lack of improvement in overcoming drug resistance with NPs was attributed to reduced endocytosis. Besides, reduced endocytosis was reported in both doxorubicin-<sup>46</sup> and cisplatin-resistant cells<sup>47</sup>.

From drug delivery perspective, however, the systematic research for the effect of the NP hardness on its internalization is still lack. In this work, we use DPD simulations to investigate the effect of NP hardness on its cellular internalization. In order to simulate different hardness NPs, we design three simple models, including polymeric NP which is built by a backbone chain grafted with short branched chains, liposome, and solid NP, as in NP-based drug formulations. The aim of this work is to highlight the importance of NP hardness on its internalization mechanism, which can provide the guidance for the design of effective NP-based drug carriers.

## 2. Models and simulation method

The DPD method has been extensively used to simulate the hydrodynamic behavior of complex fluids,<sup>48,49</sup> in which the dynamics of DPD beads are governed by Newton's equation of motion. DPD is one of the most commonly used computer simulation techniques in the studies of biomembrane systems.<sup>14, 50-58</sup> It can reproduce the dynamic behaviors of a lipid bilayer, and is often used to explore interactions between the biomembranes and NPs.<sup>7, 14, 15, 35</sup>

In this work, the coarse grained models were used to represent different components, and a schematic drawing of the studied system is given in Fig. 1. To represent dimyristoylphosphatidylcholine (DMPC), a model lipid molecule<sup>59</sup> is built

by connecting a headgroup with three hydrophilic beads (H) to two hydrophobic tails of equal length, each having five hydrophobic beads (T) (Fig. 1). The lipid membrane is composed by two types of lipid molecules with the same structure. One represents normal lipid molecules and the other represents receptors (R). In this work, we set 1/4 of lipid molecules in the membrane to behave as receptors so that the endocytosis is not receptor-limited.<sup>60</sup>

In order to investigate the effects of NP hardness on their internalization pathways, three simplified models have been design: polymeric NP, liposome, solid NP (see Fig. 1), with increasing hardness. For polymeric NP, it is built by a backbone chain and connected with many branched chains. The liposome model is obtained via a self-assembly process after connecting the beginning and the end of the polymeric NP. In the liposome model, NP deformation and shape change are allowed. Then the solid NP model is obtained by removing all bonds in the liposome and fixing its structure as a rigid solid. In this way, the polymeric NP, liposome and solid NPs have the identical hydrophilic and hydrophobic (P) components. To represent the ligand-receptor interaction, we chose hydrophilic segments (beads) of these NPs as ligands (L), which exert attractive interaction to the receptors on the membrane. The solvent molecules (W) are modeled as single beads. In order to test the efficiency of the NP carrying drug, the drug molecules (D) are also included in this work and modeled as single beads.

The interaction force exerted on beads is composed of conservative, dissipative, and random forces. The conservative force between beads  $i$  and  $j$ , which is soft and repulsive, is determined by

$$F_{ij}^C = a_{ij} \hat{r}_{ij} \max \left\{ 1 - \frac{r_{ij}}{r_c}, 0 \right\}, \quad (1)$$

where  $a_{ij}$  is the maximum repulsive force between particles  $i$  and  $j$ ,  $\mathbf{r}_{ij} = \mathbf{r}_j - \mathbf{r}_i$  ( $\mathbf{r}_i$  and  $\mathbf{r}_j$

are the positions of particle  $i$  and particle  $j$ ),  $r_{ij}=|\mathbf{r}_{ij}|$ ,  $\hat{\mathbf{r}}_{ij}=\mathbf{r}_{ij}/|\mathbf{r}_{ij}|$ , and  $r_c$  is the cutoff radius. In this system, the interaction parameters between beads of the same type were set to  $a_{TT}=15$  and  $a_{WW}=a_{HH}=a_{DD}=25$ , and those between the different types of beads were  $a_{HW}=a_{LH}=a_{LW}=a_{TP}=25$ ,  $a_{PH}=a_{PT}=a_{HT}=a_{DL}=50$ ,  $a_{LT}=a_{PW}=a_{TW}=80$ ,  $a_{HD}=a_{RD}=a_{DW}=30$ . The interaction parameters greater than 25 correspond to a repulsive force, while those smaller than 25 correspond to attraction. In order to represent the strong ligand-receptor binding, the interaction parameter between ligands and headgroups of receptors was set to zero.<sup>14</sup> As usual, we have chosen the interaction cutoff radius  $r_c$ , the bead mass  $m$ , and the thermostat temperature  $k_B T$  to unity in the simulations.

In the model of lipid molecules, the interaction between neighboring beads along the same molecule is described by a harmonic spring force,

$$F_S = K_S(r_{ij} - r_{eq})\hat{r}_{ij} \quad (2)$$

where the spring constant  $K_S$  was set to  $128k_B T$  and the equilibrium bond length  $r_{eq}$  was set to  $0.7r_c$ . The force constraining the variation of bond angle is given by

$$F_\phi = -\nabla U_\phi \quad \text{and} \quad U_\phi = K_\phi(1 - \cos(\phi - \phi_0)) \quad (3)$$

where  $\phi_0$  was set to  $\pi$  and  $K_\phi$  is the bond bending force constant. For lipid molecules and receptors,  $K_\phi$  were set to 10.0. For polymeric NP and liposome,  $K_\phi$  were set to 100.0.

In this work, we used an N-varied DPD method, a particular variant of DPD method in which the targeted membrane tension is maintained by monitoring the number of lipids per area (LNPA) in the boundary region,<sup>14, 15, 35</sup> to simulate internalization process. In this method, the boundary region which surrounds the

central square region of the membrane plays a role as a reservoir of lipids and receptors, and the value of LNPA in the boundary region (denoted as  $\rho_{LNPA}^{BR}$ ) is kept constant by deletion/addition moves. At the same time, a corresponding number of water beads are randomly deleted or added to keep the whole system density unchanged.

Since the membrane tension is directly related to  $\rho_{LNPA}^{BR}$ , we specified the value of  $\rho_{LNPA}^{BR}$  hereafter. To promote the efficiency of NP endocytosis, for most cases in this work  $\rho_{LNPA}^{BR}$  was greater than 1.47, which corresponds to zero or negative membrane tension. For the biological relevance, the negative membrane tension can be imposed by the cytoskeleton<sup>61-64</sup> or dynamin.<sup>64</sup> It is widely accepted that in many cells, actin patches assembled from actin filaments provide the driving force for the internalization of NPs.<sup>64</sup>

### 3. Results and discussion

#### 3.1 The endocytosis for NPs having different hardness

##### 3.1.1 Polymeric NP

We first considered the polymeric model that can be deformed freely, representing the softest NP. To accelerate the endocytosis kinetics, unless pointed out, a rather negative membrane tension ( $\rho_{LNPA}^{BR}=1.67$ ) was used in following simulation runs. Initially, we placed the polymeric NP close to the lipid membrane. From the typical snapshots in endocytosis process (Fig. 2a), we can see that at first the polymeric NP gradually adheres on the membrane because of the receptor and ligands attractive interaction. At the same time the polymeric NP gradually aggregates due to

the hydrophobic interaction, and at about 1280 ns the polymeric NP shrinks into a roughly spherical cluster. During the adhesion and aggregation process, the deformation of the polymeric NP is very obvious. In order to give a quantitative description for the polymeric NP deformation, we show the ellipsoidal parameter of NP in the Fig. 3a, which is defined as  $E = H / W$  with  $H$  and  $W$  the height and width of the NP. With further proceeding, all the ligands are pulled to the membrane surface owing to the ligand-receptor attractive interaction, resulting in the absence of ligands on the top of the polymeric NP that blocks further wrapping. The observation confirms that the uniform distribution of ligands on NP surfaces is crucial for successful endocytosis. For soft NPs, however, the ligands would gradually diffuse to the NP-membrane interface to bind with the receptors. As a result, the wrapping rate slows down and finally stops as the depletion of free ligands, which leads to the failure of endocytosis.

Besides, we also explored the effect of membrane surface tension by considering respectively a positive membrane tension ( $\rho_{LNPA}^{BR}=1.25$ ), a zero membrane tension ( $\rho_{LNPA}^{BR}=1.47$ ) and a negative membrane tension ( $\rho_{LNPA}^{BR}=1.67$ ). Generally, the positive membrane tension would lengthen the wrapping stage and consequently slows down the wrapping kinetics. A small or negative membrane tension would facilitate the NP wrapping, and always generates a large membrane curvature to wrap the NP (Fig. 4). In general the decrease of membrane tension would promote the membrane bending to wrap the polymeric NP. However, even though at the negative membrane tension, the mobility of ligands on a soft NP would cause the depletion of free ligands at the

last wrapping stage that prevents full endocytosis of the polymeric NP (Fig. 4a).

The mechanism for the frustrated endocytosis of the polymeric NP can be used to interpret the fact that although some soft biomacromolecules such as charged DNA, proteins, filaments<sup>65</sup> may show attractive interaction with the cell membrane, they still cannot be endocytosed. One of the important reasons is that soft biomacromolecule cannot keep the uniform distribution of their “ligands” during a whole internalization process. The absence of the free “ligands” at the last stage will limit the endocytosis of macromolecules.

### 3.1.2 Liposome

We show typical the time evolution of the wrapping of liposome in Fig.2b. From Fig.2b, we can see that as the wrapping process proceeds, the ligands on the top of the liposome gradually move to the membrane surface to interact with the receptors on the membrane. Finally, the absence of ligands on the top of the liposome inhibits its full endocytosis, in a similar manner as for the polymeric NP. Besides, with being wrapped by lipid membrane, liposome deform into a shape of oblate spheroid due to the strong ligand-receptor attraction (see Fig. 3a).

We also studied the effect of membrane tension on the endocytosis. Fig. 4b shows the final snapshots for liposome wrapped at different membrane tensions. Besides, we give the time evolution of wrapping percentage in Fig. 5a. The figures show that at positive membrane tension ( $\rho_{LNPA}^{BR}=1.25$ ) or zero membrane tension ( $\rho_{LNPA}^{BR}=1.47$ ), the liposome is hardly wrapped by the membrane, and instead the NP is

strongly deformed to maximize the ligand-receptor interaction. Even at the negative surface tension ( $\rho_{LNPA}^{BR}=1.67$ ), NP softness induced NP deformation and depletion of free ligands prevent the NP from being full wrapped by the membrane. Similar results were found by Ding and Ma on the NP-membrane interaction<sup>30</sup> as well as by us on the vesicle-membrane interaction,<sup>35</sup> indicating that depletion of free ligands and shape change of soft NPs induce frustrated internalization.

### 3.1.3 Solid NP

To compare with the engulfment of soft NPs, we also investigated the endocytosis of solid spherical NP at a negative membrane tension of  $\rho_{LNPA}^{BR}=1.67$ . As shown in Fig.2c, the solid NP can be endocytosed completely. During the endocytosis process, the solid NP was first adhered and then gradually wrapped by the lipid membrane until it was internalized fully. Compared to the soft NP under the same conditions, the solid NP can keep the roughly uniform distribution of ligands during the endocytosis process. This is one of the key reasons that solid sphere NP can be endocytosed, but soft NPs can not.

In addition, we also show the effect of membrane tension on the endocytosis of solid NPs in Fig. 4c and Fig. 5b, in which the positive membrane tension would lengthen the wrapping stage, and consequently the kinetics of endocytosis slows down. In contrast, a small or negative membrane tension facilitates the generation of a large membrane curvature and promotes the endocytosis of the solid NP.

### ***3.2 The mechanism for soft nanoparticle cannot endocytosis***

The mechanism of selective control of endocytosis by tailoring NP hardness can be interpreted by two aspects. One is the depletion rate of free ligands relative to the wrapping process, and the other is the shape deformation of NPs.

#### ***3.2.1 The change of ligand distribution during a wrapping process***

For soft elastic NPs such as polymeric NP and liposomes, when they absorbed on a lipid membrane, receptors adjacent to the soft NP can diffuse to form strong binding with the mobile ligands on the NP, which causes the anisotropy of ligand distribution. At the last stage of the wrapping process the free ligands are depleted, and therefore, the absence of ligands on the top of the soft elastic NP will limit its further endocytosis. In order to further explore the importance of surface ligand distribution in successful endocytosis, we investigated another system in which the interaction among ligands on the liposome becomes repulsive in order to constrain the free motion of ligands and prevent their strong enrichment on the NP-membrane interface. We call the soft NP as “dendrimer”. Note that these kind of soft NPs do certainly not have a structure of dendrimers, but they behave as dendrimers during a wrapping process. They do constrain the local enrichment of ligands on the NP-membrane interface as dendrimer, in which the volume repulsion induces a constraint on free motion of ligands that generates a relatively uniform ligand distribution during the wrapping process ( $a_{LL} = 50$ ).

From the Fig.6, we can see that the dendrimer-like NP does prevent the rapid

depletion of free ligands during the first stage of the wrapping process. Compared to the liposome, therefore, the “dendrimer” has a larger wrapping percentage (Fig. 5c). This further confirms that a slow depletion rate of free ligands relative to the wrapping is one of necessary conditions for NP endocytosis. Especially, it was experimentally found that mobile ligands tend to redistribute in the response to the change in the local environment.<sup>66</sup>

### ***3.2.2 The shape deformation of a soft NP***

The deformation of the soft NP in the wrapping process is another key factor affecting NP endocytosis. In order to study the effects of the deformation of NPs having different hardness in their wrapping process, we compared the endocytosis of the “dendrimer” with the solid spherical NP. For the solid spherical NP, it shows a slight rotation during the endocytosis process as the NP is not a strict sphere (Fig. 3a). As a result, the ellipsoidal parameter of the solid NP shows a slight fluctuation. However, the ellipsoidal parameter of the “dendrimer” shows a much more significantly decrease at the early stage and then increases as the simulation time proceeds (see Fig. 3b). This means that at the early stage the “dendrimer” first spread out on the lipid membrane to maximize the ligand-receptor attraction. Fig. 5c shows that the endocytosis kinetics of the “dendrimer” is slower than the solid sphere NP, indicating that the shape deformation of the “dendrimer”, especially for the first one, is not favorable for its wrapping.

At the later stage, as the ligand-receptor attraction is sufficiently strong to

compensate the cost of membrane bending, the membrane bends and more free ligands move to interact with the membrane. Consequently, the wrapping rate for the “dendrimer” increases at this stage (Fig. 5c). At the same time, the “dendrimer” deforms into a slender sphere (Fig.6, Fig. 3b).

In general, the endocytosis of “dendrimer” is much slower in comparison with the solid spherical NP. This is because the shape deformation of soft NPs is not favorable for its wrapping (Fig. 3b, Fig.5c). Therefore, our results show that even if the “dendrimer” can slow down the depletion of free ligands in some extent, its shape deformation during a wrapping process is unfavorable for NP endocytosis when compared to the solid spherical NP.

### ***3.3 The penetration pathways for soft NPs carrying drug molecules***

In experiments, liposomes including micelles or vehicles are often used as nanocarrier for drug and gene delivery.<sup>39</sup> In order to study how soft liposomes carrying drug enter the cell, we study the dynamics mechanism for drug-carrying liposome entering into cells. At first, the hydrophobic drug molecules are encapsulated inside a liposome. Then, we placed the liposome near a lipid membrane to simulate the drug delivery process. Several final configurations are shown in Fig.7.

Our simulations show that the fate of liposomes depends on the interaction between the hydrophobic segments of liposomes and lipid tails. As the interaction gradually decreases from repulsion to attraction, liposomes respond to the liposome-membrane attraction differently, showing interaction pathways from NP

adhesion and penetration. At  $a_{PT}=50$ , the liposomes are found to stay adhering on the membrane, being wrapped partially by the membrane during their interaction process (see Fig. 7a). This observation is in a good agreement with Fig. 2b. In general, for soft NPs under the endocytosis pathway, most frequently the liposome cannot be fully wrapped by the lipid membrane, leading to the failure of transporting drug molecules into cells.

When the interaction between liposome and membrane hydrophobic beads showing weak or zero repulsion, such as  $a_{PT}=25$ , soft NPs tend to merge with a bilayer membrane via rearranging their hydrophobic and hydrophilic segments, inducing NP penetration (Fig.7b). Therefore, the endocytosis pathway can be blocked via weakening the repulsive interaction between the liposome hydrophobic segment and the lipid tails. In this case the liposome is found to enter the lipid membrane with a penetration pathway instead. Besides, it is interesting to find that the penetration of liposomes has three different pathways (see Fig. 8 for typical snapshots).

For the penetration of the liposome, we found three penetration mechanisms: “fusion-wrapping-switch” mechanism, “fusion-penetration-rearrangement” mechanism, and “fusion-hydrophobic insertion” mechanism. For the “fusion-wrapping-switch” mechanism, it is initiated from the fusion of the soft NP with the membrane (Fig. 8a), just as in the membrane fusion events discussed for micelle<sup>67</sup> and vesicles.<sup>35,51</sup> During the membrane fusion, hydrophobic segments at the bottom of the liposome tend to penetrate into the membrane hydrophobic core, and at the same time the liposome ligands are pushed away and concentrate on the top of the

liposome, which consequently induces a stronger attraction between the liposome and receptors in the membrane and thus enhances the NP wrapping as in a pinocytosis pathway. As the whole liposome gradually immerses into the membrane, a hydrophobic-hydrophilic switch, in which the liposome gradually extends its hydrophobic segments outward and forms a hydrophobic shell wrapping the hydrophilic segments, takes place to minimize the contact between neighboring beads having different hydrophobicity, forming an inverted micelle-like structure (Fig. 8a). We must notice that in our simulations the NP size is rather small and comparable with the membrane thickness. For soft NPs with a much larger size, the wrapping process of the penetration pathways may become a limited step.

Another penetration pathway for the liposome is called “fusion-penetration-rearrangement” mechanism, in the case of drug molecules having a strong attraction with the liposome (Fig.8b). Different from the first penetration pathway, in this pathway the liposome along with its hydrophilic beads can directly penetrate the lipid membrane with less segment rearrangement, like the direct penetration of patterned solid NPs<sup>68</sup> and the dendrimer-induced formation of membrane pore.<sup>69</sup> Since some hydrophilic segments of the liposome (ligands) contact with the hydrophobic core of the lipid membrane directly after the soft NP reaches the other leaflet of the membrane, this pathway is followed by the rearrangement of liposome beads to minimize the unfavorable hydrophobic-hydrophilic contact. The final configuration in Fig. 8b shows that the whole liposome forms a hydrophilic-hydrophobic-hydrophilic structure inside the membrane, as the interaction

of patterned solid NP with cellular membrane.<sup>68</sup>

The third penetration pathway for the liposome is “fusion-hydrophobic insertion” mechanism (Fig.8c). In this pathway, the hydrophobic segments of the liposome gradually insert into the membrane after the initial fusion of NP with the membrane. But different from the “fusion-penetration-rearrangement” mechanism, the hydrophilic beads of the liposome on the upper leaflet could not reach the lower leaflet (see Fig. 8c).

### 3.4 NP-drug molecule attraction influences the efficiency of drug delivery

Besides, we found that the penetration pathway for the liposome is also dependent upon the interaction between the liposome and drug molecules. When the drug molecules are of strong attraction with the hydrophobic segment of the liposome (e.g.,  $a_{PD} = 0$ ), the liposome penetrates mainly via the “fusion-penetration-rearrangement” pathway. This is because the strong drug-liposome attraction effectively rigidifies the liposome, resulting in NP penetration as patterned solid NP.<sup>68</sup> Whereas, when the interaction between the hydrophobic segment of the liposome and the drug becomes increasingly weak ( $a_{PD} = 10$  and then  $a_{PD} = 25$ ), the penetration of the liposome is dominated mainly by the “fusion-wrapping-switch” pathway and then the “fusion-hydrophobic insertion” pathway.

At the same time, our simulations demonstrate that the attractive interaction between the drug molecules and liposome also influences the efficiency of drug delivery via changing drug release. For soft NPs having a zero or weak attraction with

the drug molecules, the deformation of soft NPs, which is observed in both the endocytosis (Fig. 7a) and penetration pathways (Fig. 7b), could lead to the leakage of drug molecules before their internalization. Consequently, a large number of drug molecules fail to cross the lipid membrane and weakens the drug delivery efficiency (see Fig.7c, and Fig. 7d). However, if there has a strong attraction between the drug molecules and soft NPs, drug leakage before NP uptake can be substantially reduced (see Fig.7e).

In general, the attraction between the drug molecules and liposome not only inhibits the leakage of the drug molecules, but also changes effectively the NP hardness and the penetration pathways. Hence, when soft NPs are selected as nanocarriers for drug delivery, it should keep in mind that besides the NP-membrane interaction, the NP-drug molecule interaction is also important for effective drug delivery. An appropriate choice of the interaction between drug and soft NPs can avoid substantial drug release of ahead of their internalization.

#### **4. Conclusions**

Nanoparticles (NPs) have shown significant promise in development of drugs delivery systems that might overcome the limitations of current therapeutic agents. For example, various NP-based approaches have been investigated to overcome the multidrug resistance developed by tumor cells. However, in many cases the inefficient internalization of the nanocarriers is often one of major sources for drug resistance, and the poor cellular uptake remains the rate-limiting step for NP-based drug delivery

systems.

NPs can be categorized with respect to their hardness or softness, and how NP hardness influence the drug delivery is nearly unexplored. In this work, we used the dissipative particle dynamics simulation to investigate how to control selectively internalization pathway by tailoring NP hardness. Different simplified models for platforms used for drug delivery, including polymeric NP, liposome, dendrimer, and solid NP are considered here to represent the increase of nanocarrier hardness. Our simulation results indicate that without the aid of other cellular machineries, only rigid NPs can achieve complete endocytosis. For the polymeric NP, liposome and even the dendrimer, however, the endocytosis process can be inhibited or frustrated. There are mainly two reasons for the endocytic difficulty of soft elastic NPs. One is rapid depletion of free ligands on the top of soft NPs that limits further wrapping process. The other is the shape deformation of the soft NPs induced by the ligand-receptor attraction, which slows down the wrapping process.

Instead, soft NPs are often found to enter the lipid membrane with a penetration pathway via rearranging their hydrophobic and hydrophilic segments. Our simulation results show that there exist three different penetration pathways: “fusion-wrapping-switch” mechanism, “fusion-penetration-rearrangement” mechanism, and “fusion-hydrophobic insertion” mechanism. The fate of internalization of soft NPs depends on the interaction between the hydrophobic segments of liposomes and lipid tails. Besides, the pathway for the penetration of soft NPs is affected by the attractive interaction between the drug molecules and NPs.

Finally, we show that the drug delivery efficiency of soft NPs not only depends on their ability to be internalized, but depends on the interaction between the carriers and drug molecules. A weak attraction between soft NP and drug molecules could lead to the leakage of drug molecules before their internalization. In contrast, for soft nanocarriers with a strong attraction with drug molecules, drug leakage before NP uptake can be substantially reduced.

This work gives a comprehensive explanation of how the NP hardness influence on their internalization pathway, which can give some guidance for the design of drug delivery systems. Besides NP hardness, other principles for the design of soft nanocarriers can also be derived from our simulations. For example, the interaction between the hydrophobic segments of soft NPs and lipid tails is essential for the successful penetration of soft NPs. In addition, the interaction between the soft carriers and drug molecules also affects the drug loading capacity, although its influence on the ratio of NP uptake is negligible.

### **Acknowledgements**

This work is supported by National 973 Program (2011CB706900), NSF of China (91334203, 21274011, 21276007), University Scientific Research Funding (ZZ1304) and Excellent Talent (RC1301) of BUCT.

## References

- 1 Q. Yin, J. Shen, Z. Zhang, H. Yu, Y. Li, *Adv. Drug Del. Rev.*, 2013, **65**, 1699-1715.
- 2 C. Bock, T. Lengauer, *Nature Reviews Cancer*, 2012, **12**, 494-501.
- 3 X.-J. Liang, C. Chen, Y. Zhao, P. C. Wang, *Methods in molecular biology (Clifton, N.J.)*, 2010, **596**, 467-88.
- 4 C. Peetla, S. Vijayaraghavalu, V. Labhasetwar, *Adv. Drug Del. Rev.*, 2013, **65**, 1686-1698.
- 5 A. R. Kirtane, S. M. Kalscheuer, J. Panyam, *Adv. Drug Del. Rev.*, 2013, **65**, 1731-1747.
- 6 S. Pogodin, M. Werner, J.-U. Sommer, V. A. Baulin, *ACS nano*, 2012, **6**, 10555-10561.
- 7 K. Yang, Y.-Q. Ma, *Nat. Nanotechnol.*, 2010, **5**, 579-583.
- 8 A. Verma, O. Uzun, Y. Hu, Y. Hu, H.-S. Han, N. Watson, S. Chen, D. J. Irvine, F. Stellacci, *Nat. Mater.*, 2008, **7**, 588-595.
- 9 S. Hong, A. U. Bielinska, A. Mecke, B. Keszler, J. L. Beals, X. Shi, L. Balogh, B. G. Orr, J. R. Baker, M. M. Banaszak Holl, *Bioconjugate Chem.*, 2004, **15**, 774-782.
- 10 X. Shi, A. von Dem Bussche, R. H. Hurt, A. B. Kane, H. Gao, *Nat. Nanotechnol.*, 2011, **6**, 714-719.
- 11 P. Decuzzi, M. Ferrari, *Biomaterials*, 2007, **28**, 2915-2922.
- 12 H. Gao, W. Shi, L. B. Freund, *Proceedings of the National Academy of Sciences of the United States of America*, 2005, **102**, 9469-9474.
- 13 J. Rejman, V. Oberle, I. S. Zuhorn, D. Hoekstra, *Biochem. J.*, 2004, **377**, 159.
- 14 T. Yue, X. Zhang, *Soft Matter*, 2011, **7**, 9104-9112.
- 15 T. Yue, X. Zhang, *ACS nano*, 2012, **6**, 3196-3205.
- 16 B. J. Reynwar, G. Illya, V. A. Harmandaris, M. M. Müller, K. Kremer, M. Deserno, *Nature*, 2007, **447**, 461-464.
- 17 S. Zhang, J. Li, G. Lykotrafitis, G. Bao, S. Suresh, *Adv. Mater.*, 2009, **21**, 419-424.
- 18 H. Yuan, S. Zhang, *Appl. Phys. Lett.*, 2010, **96**, 033704.
- 19 B. D. Chithrani, A. A. Ghazani, W. C. Chan, *Nano Letters*, 2006, **6**, 662-668.
- 20 B. D. Chithrani, W. C. Chan, *Nano Letters*, 2007, **7**, 1542-1550.
- 21 W. Jiang, B. Y. Kim, J. T. Rutka, W. C. Chan, *Nat. Nanotechnol.*, 2008, **3**, 145-150.
- 22 I. Slowing, B. G. Trewyn, V. S.-Y. Lin, *J. Am. Chem. Soc.*, 2006, **128**, 14792-14793.
- 23 S. H. Kim, J. H. Jeong, K. W. Chun, T. G. Park, *Langmuir*, 2005, **21**, 8852-8857.
- 24 H. Yuan, J. Li, G. Bao, S. Zhang, *Phys. Rev. Lett.*, 2010, **105**, 138101.
- 25 E. H. Shin, Y. Li, U. Kumar, H. V. Sureka, X. Zhang, C. K. Payne, *Nanoscale*, 2013, **5**, 5879-5886.
- 26 A. Villanueva, M. Canete, A. G. Roca, M. Calero, S. Veintemillas-Verdaguer, C. J. Serna, M. del Puerto Morales, R. Miranda, *Nanotechnology*, 2009, **20**, 115103.
- 27 E. C. Cho, J. Xie, P. A. Wurm, Y. Xia, *Nano Letters*, 2009, **9**, 1080-1084.
- 28 O. Harush-Frenkel, E. Rozentur, S. Benita, Y. Altschuler, *Biomacromolecules*, 2008, **9**, 435-443.
- 29 R. C. Van Lehn, A. Alexander-Katz, *Soft Matter*, 2014, **10**, 648-658.
- 30 H. Ding, Y. Ma, *Biomaterials*, 2012, **33**, 5798-5802.
- 31 S. L. Tao, T. A. Desai, *J. Controlled Release*, 2005, **109**, 127-138.
- 32 K. A. Beningo, C.-M. Lo, Y.-L. Wang, *Methods in cell biology*, 2002, **69**, 325-339.
- 33 X. Yi, X. Shi, H. Gao, *Phys. Rev. Lett.*, 2011, **107**, 098101.
- 34 X. Yi, H. Gao, *Phys. Rev. E*, 2014, **89**, 062712.

- 35 T. Yue, X. Zhang, *Soft Matter*, 2013, **9**, 559-569.
- 36 A. V. Kabanov, E. V. Batrakova, V. Y. Alakhov, *Adv. Drug Del. Rev.*, 2002, **54**, 759-779.
- 37 E. V. Batrakova, A. V. Kabanov, *J. Controlled Release*, 2008, **130**, 98-106.
- 38 Y. Kakizawa, K. Kataoka, *Adv. Drug Del. Rev.*, 2002, **54**, 203-222.
- 39 A. Misra, K. Jinturkar, D. Patel, J. Lalani, M. Chougule, *Expert Opinion on Drug Delivery*, 2009, **6**, 71-89.
- 40 Y.-C. Tseng, S. Mozumdar, L. Huang, *Adv. Drug Del. Rev.*, 2009, **61**, 721-731.
- 41 W. Li, F. C. Szoka, Jr., *Pharm. Res.*, 2007, **24**, 438-449.
- 42 R. Duncan, L. Izzo, *Adv. Drug Del. Rev.*, 2005, **57**, 2215-2237.
- 43 P. P. Constantinides, M. V. Chaubal, R. Shorr, *Adv. Drug Del. Rev.*, 2008, **60**, 757-767.
- 44 M. Arruebo, R. Fernández-Pacheco, M. R. Ibarra, J. Santamaría, *Nano today*, 2007, **2**, 22-32.
- 45 S. Kunjachan, A. Blauz, D. Moeckel, B. Theek, F. Kiessling, T. Etrych, K. Ulbrich, L. van Bloois, G. Storm, G. Bartosz, B. Rychlik, T. Lammers, *Eur. J. Pharm. Sci.*, 2012, **45**, 421-428.
- 46 T. Takahashi, T. Furuchi, A. Naganuma, *Cancer Res.*, 2006, **66**, 11932-11937.
- 47 D. W. Shen, A. Su, X. J. Liang, A. Pai-Panandiker, M. M. Gottesman, *Br. J. Cancer*, 2004, **91**, 270-276.
- 48 P. Espanol, P. Warren, *EPL (Europhysics Letters)*, 1995, **30**, 191.
- 49 P. Hoogerbrugge, J. Koelman, *EPL (Europhysics Letters)*, 1992, **19**, 155.
- 50 M. Venturoli, B. Smit, M. M. Sperotto, *Biophys. J.*, 2005, **88**, 1778.
- 51 J. C. Shillcock, R. Lipowsky, *Nat. Mater.*, 2005, **4**, 225-228.
- 52 S. Li, X. Zhang, W. Wang, *Biophys. J.*, 2010, **98**, 2554-2563.
- 53 S. Li, X. Zhang, W. Wang, *J. Phys. Chem. B*, 2009, **113**, 14431-14438.
- 54 T. Yue, S. Li, X. Zhang, W. Wang, *Soft Matter*, 2010, **6**, 6109-6118.
- 55 L. Gao, R. Lipowsky, J. Shillcock, *Soft Matter*, 2008, **4**, 1208-1214.
- 56 M. Laradji, P. Sunil Kumar, *Phys. Rev. Lett.*, 2004, **93**, 198105.
- 57 U. Schmidt, G. Guigas, M. Weiss, *Phys. Rev. Lett.*, 2008, **101**, 128104.
- 58 A. Alexeev, W. E. Uspal, A. C. Balazs, *ACS nano*, 2008, **2**, 1117-1122.
- 59 F. J.-M. De Meyer, M. Venturoli, B. Smit, *Biophys. J.*, 2008, **95**, 1851-1865.
- 60 Y. Li, T. Yue, K. Yang, X. Zhang, *Biomaterials*, 2012, **33**, 4965-4973.
- 61 M. Kaksonen, C. P. Toret, D. G. Drubin, *Nature Reviews Molecular Cell Biology*, 2006, **7**, 404-414.
- 62 E. Smythe, K. R. Ayscough, *J. Cell Sci.*, 2006, **119**, 4589-4598.
- 63 J. B. Moseley, B. L. Goode, *Microbiol. Mol. Biol. Rev.*, 2006, **70**, 605-645.
- 64 G. J. Doherty, H. T. McMahon, *Annual review of biochemistry*, 2009, **78**, 857-902.
- 65 Y. Geng, P. Dalhaimer, S. Cai, R. Tsai, M. Tewari, T. Minko, D. E. Discher, *Nat. Nanotechnol.*, 2007, **2**, 249-255.
- 66 H.-Y. Lee, S. H. R. Shin, L. L. Abezgauz, S. A. Lewis, A. M. Chirsan, D. D. Danino, K. J. Bishop, *J. Am. Chem. Soc.*, 2013, **135**, 5950-5953.
- 67 J. Gao, S. Li, X. Zhang, W. Wang, *PCCP*, 2010, **12**, 3219-3228.
- 68 Y. Li, X. Zhang, D. Cao, *Soft Matter*, 2014, **10**, 6844-6856.
- 69 Y.-q. Ma, *Soft Matter*, 2012, **8**, 2627-2632.

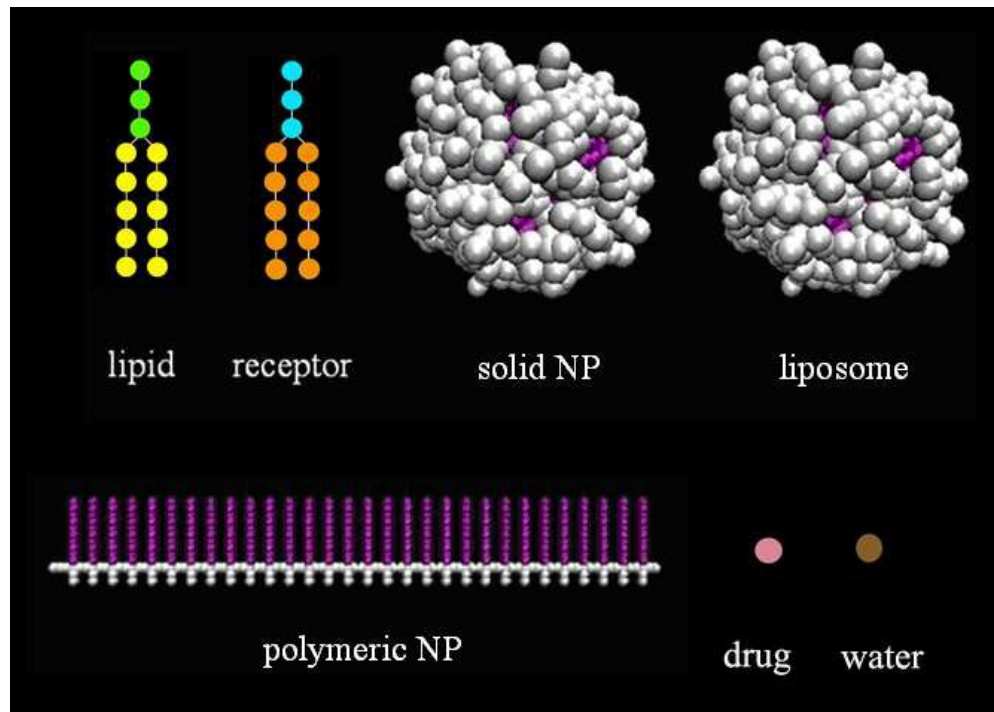


**Fig. 1.** Schematic drawing of different components in our systems. The lipid head is shown in green, lipid tail in yellow, receptor head in cyan, receptor tail in orange, water molecule in brown, and drug molecule in pink. For different NP models, the hydrophilic component is shown in white and the hydrophobic component is shown in purple.

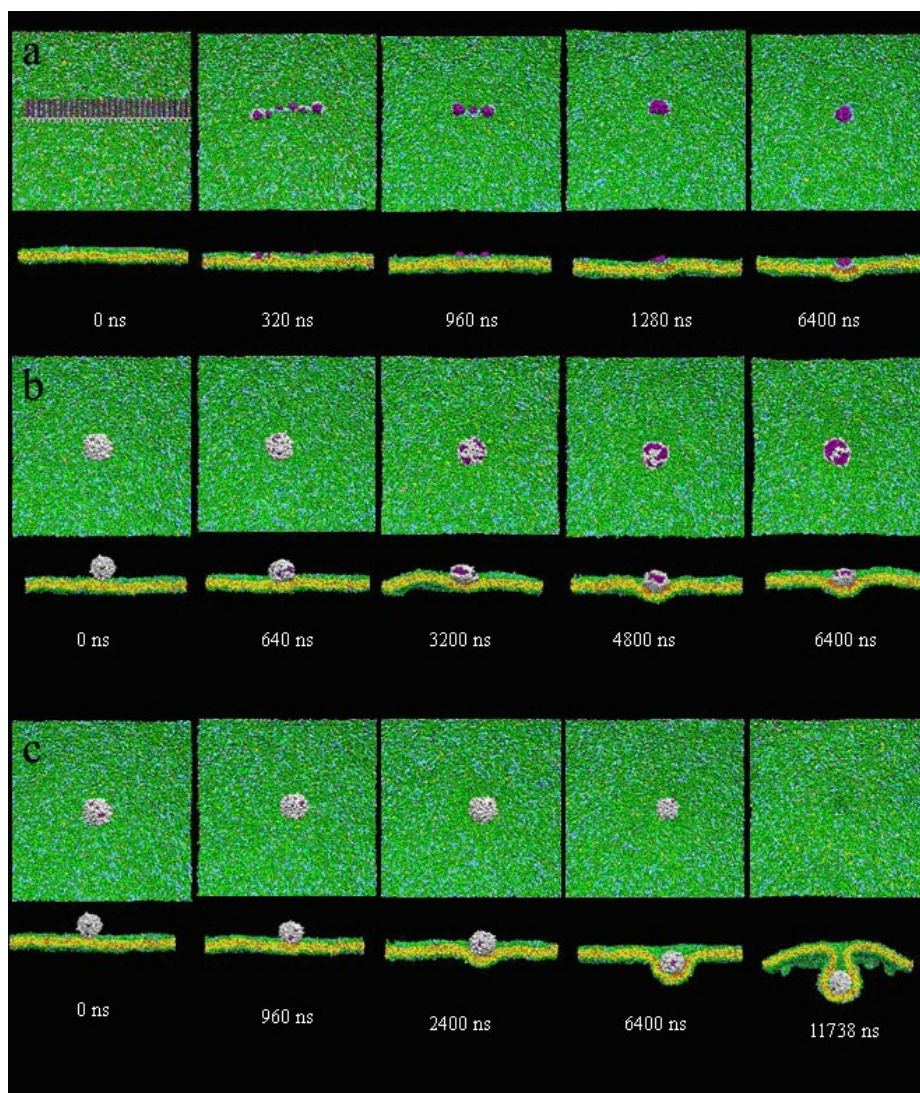


**Fig. 2.** Several typical snapshots for endocytosis processes for polymeric NP (a), liposome (b), solid NP (c). In the snapshots, the color code for the snapshots is the same as in Fig. 1. Water molecules are not shown in the snapshots for clarity. The volume of the liposome and solid NPs is  $162 \text{ nm}^3$ , whereas that for the polymeric NP is  $41 \text{ nm}^3$ .

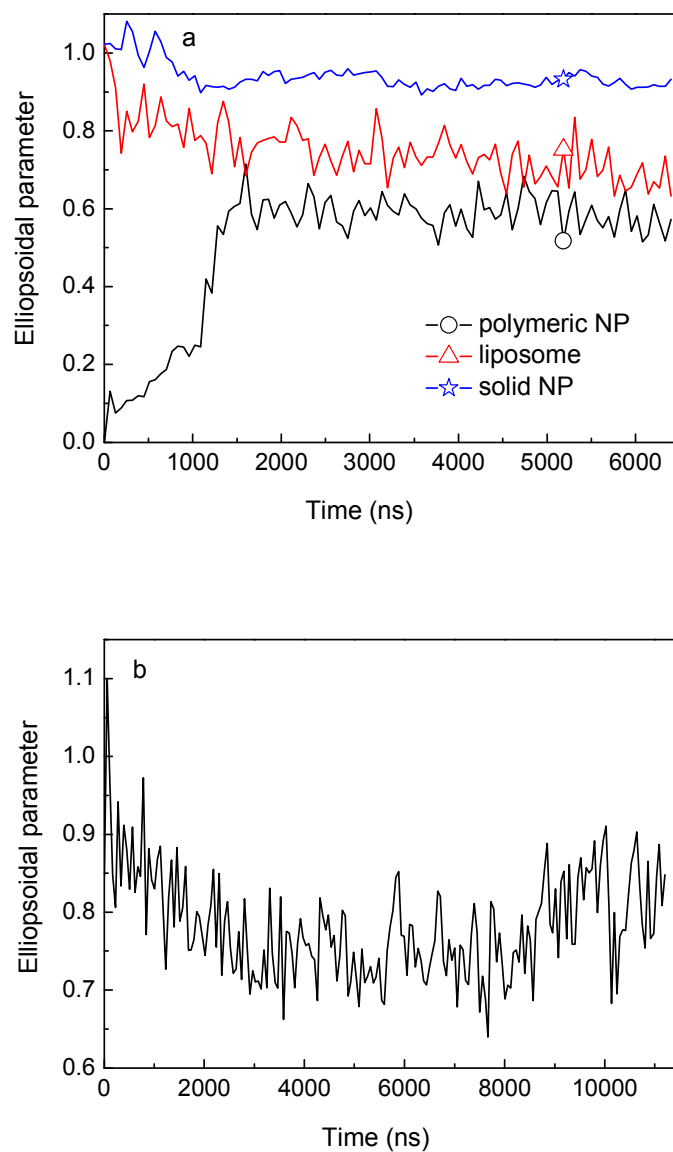


**Fig. 3.** Time evolution of the ellipsoidal parameter for the wrapping of different NPs: (a) polymeric, liposome, and solid spherical NP at  $\rho_{LNPA} = 1.67$ ; (b) “dendrimer” at  $\rho_{LNPA} = 1.67$  (dendrimer: with repulsive interaction between the neighboring ligands,  $a_{LL} = 50$ )

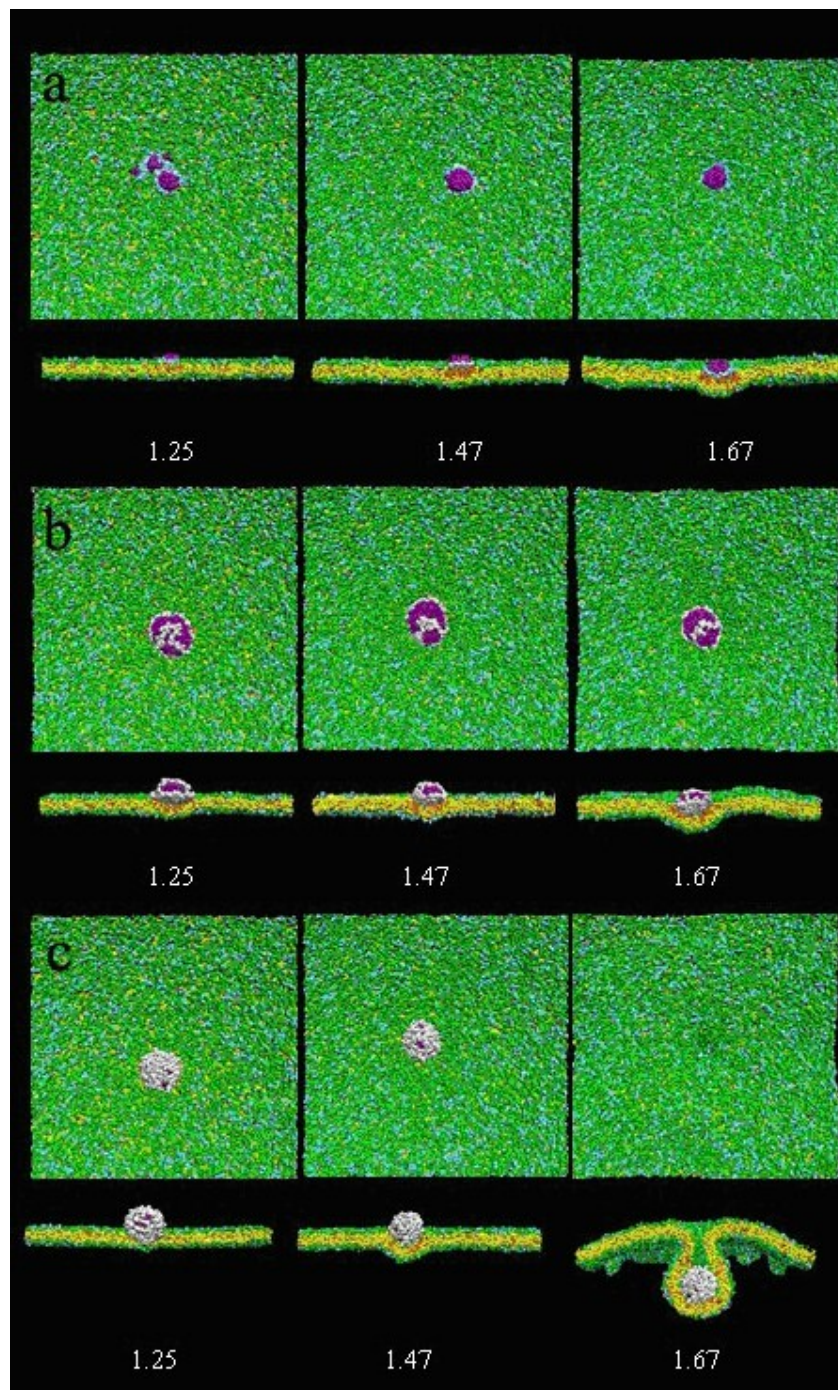


**Fig. 4.** Final configurations for the wrapping of polymeric (a), liposome (b) and solid NP (c) at  $\rho_{LNPA} = 1.25$ ,  $\rho_{LNPA} = 1.47$ , and  $\rho_{LNPA} = 1.67$ , respectively, from left to right. The color code for the snapshots is the same as in Fig. 1. The volume of the liposome and solid spherical NP is  $162 \text{ nm}^3$ , whereas that for the polymeric NP is  $41 \text{ nm}^3$ .

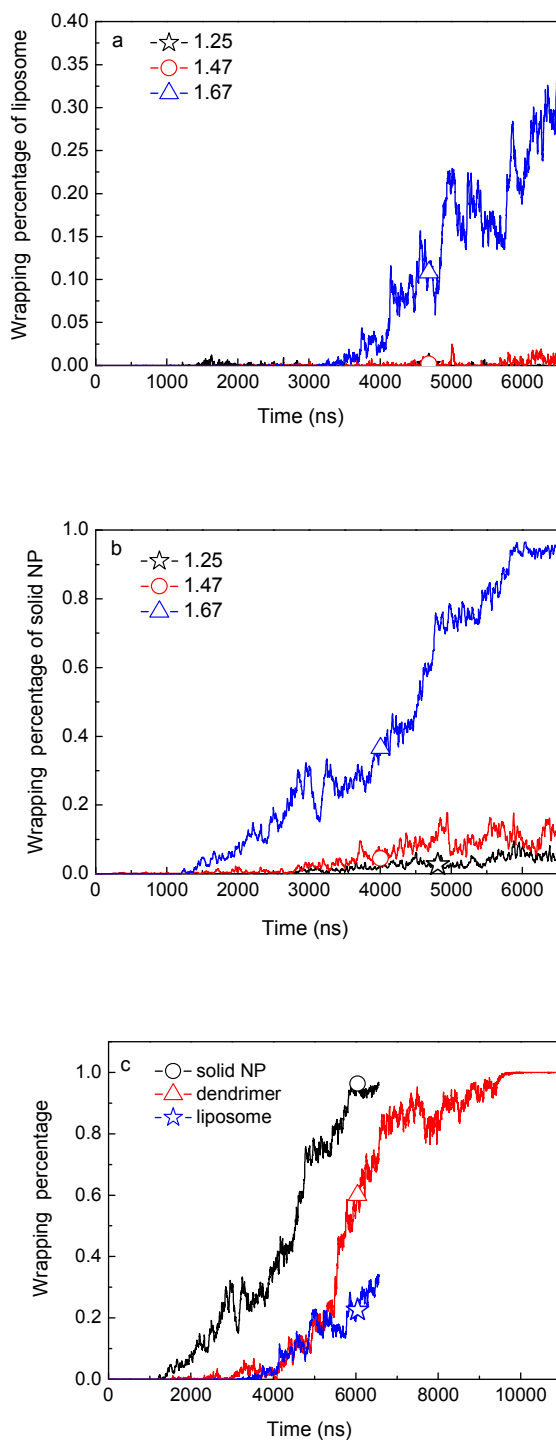


**Fig. 5.** Endocytosis kinetics of NPs: (a) liposome at  $\rho_{LNPA} = 1.25$ ,  $\rho_{LNPA} = 1.47$ , and  $\rho_{LNPA} = 1.67$ ; (b) solid NP at  $\rho_{LNPA} = 1.25$ ,  $\rho_{LNPA} = 1.47$ ,  $\rho_{LNPA} = 1.67$ ; (c) different NPs at  $\rho_{LNPA} = 1.67$  (dendrimer: with repulsive interaction between neighboring ligands.).

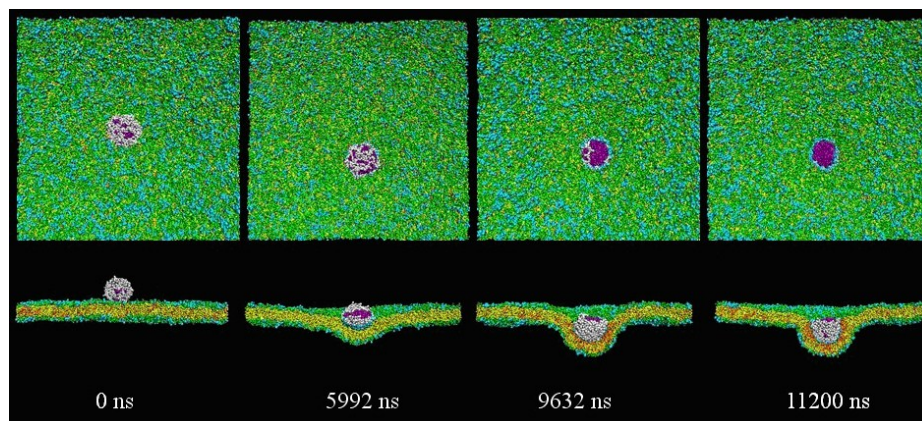


**Fig. 6.** Several typical snapshots for the wrapping process of “dendrimer” at  $\rho_{LNP} = 1.67$ . The color code for the snapshots is the same as in Fig. 1. The volume of the “dendrimer” is  $162 \text{ nm}^3$ .

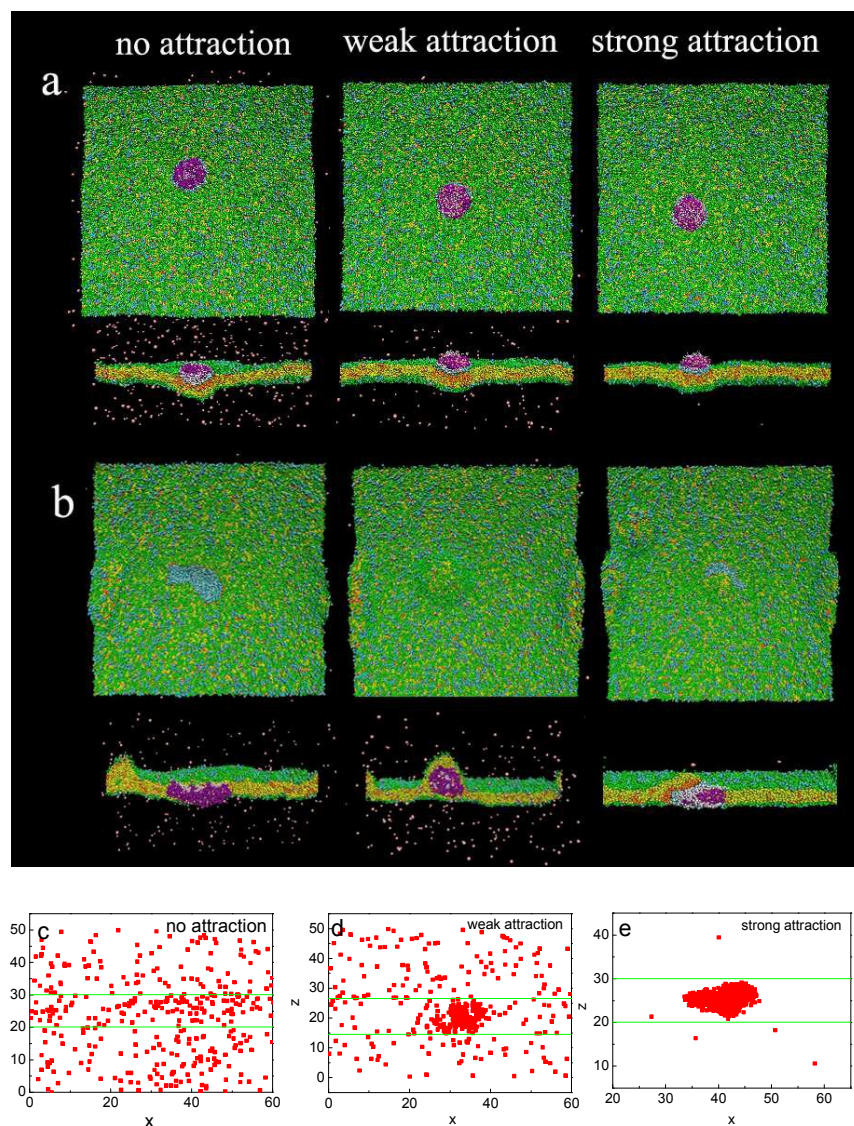
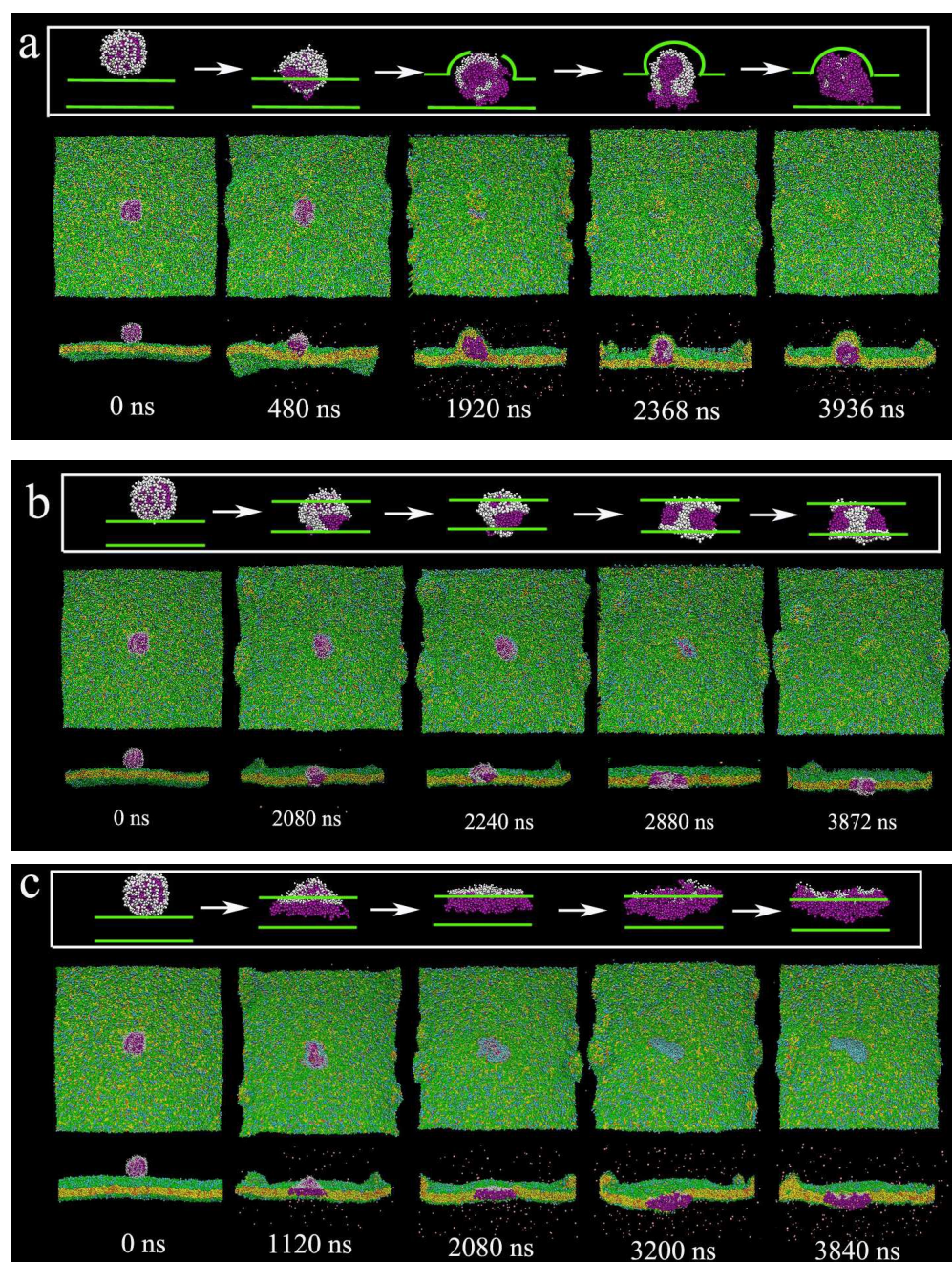


Fig. 7 The internalization of liposome carrying drug at  $\rho_{LNPA} = 1.67$ . The color code for the snapshots is the same as in Fig. 1. (a, b) show final snapshots for the fate of liposome as a function of  $a_{PT}$ : (a)  $a_{PT} = 50$ ; (b)  $a_{PT} = 25$ . (c-e) give the corresponding distributions of drug molecules in the case of  $a_{PT} = 25$ . From left to right, the interaction between liposome hydrophobic segments and drug molecules is set to  $a_{PD} = 25$  (no attraction), 10 (weak attraction), 0 (strong attraction). The green lines in (c-e) represent the top and bottom positions of lipid heads.



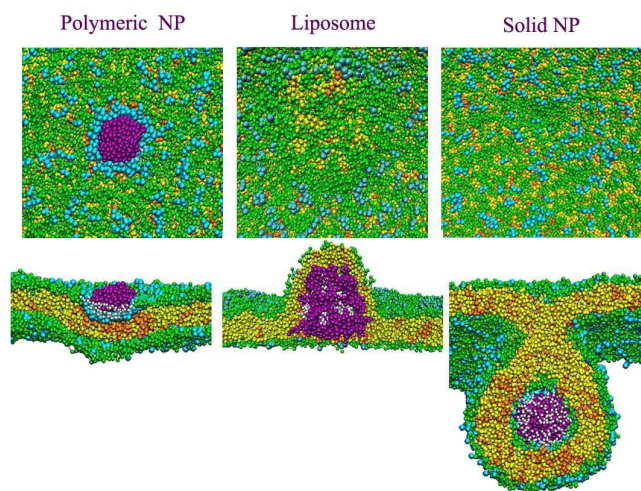
**Fig. 8.** Several typical snapshots corresponding to the three pathways for liposome penetration. The color code for the snapshots is the same as in Fig. 1.

## Table of Contents Graphics

---

### Nanoparticle Hardness Controls the Internalization Pathways for Drug Delivery

Ye Li, Xianren Zhang and Dapeng Cao



TEXT: Rigid nanoparticles may internalize with an endocytic pathway, whereas soft nanoparticles tend to find a penetration pathway to enter biomembranes.

---